9^{th} *LISA Symposium, Paris*
ASP Conference Series, Vol. 467
G. Auger, P. Binétruy and E. Plagnol, eds.

Analytic Model for the Rototranslational Torsion Pendulum

Fabrizio De Marchi,[1] Massimo Bassan,[1] Giuseppe Pucacco,[1]
Lorenzo Marconi,[2] Ruggero Stanga,[2] Massimo Visco[3]

[1]*Dipartimento di Fisica, Università di Roma Tor Vergata and INFN, Sezione di Roma Tor Vergata, I-00133 Roma*

[2]*Dipartimento di Fisica ed Astronomia, Università degli Studi di Firenze, and INFN, Sezione di Firenze*

[3]*IAPS-INAF and INFN, Sezione di di Roma "Tor Vergata", I-00133 Roma*

Abstract. We develop an analytic model to describe the motion of the RotoTranslational Torsion Pendulum PETER in a wide range of frequencies (from 1mHz up to 10-15Hz). We also try to explain some unexpected features we found in the data with only 1 soft degree of freedom and we estimate values for the misalignment angles and other parameters of the model.

Introduction. In preparation for the flight of LISA-Pathfinder (McNamara et al. 2008), a torsion pendulum is a useful tool to understand and characterize all possible sources of spurious noise that can affect the free fall of a Test Mass in geodesic motion.

To this purpose, successful pendulums have been developed in the Universities of Trento (Carbone et al. 2005, 2006) and Washington (Pollack et al. 2010), where many possible sources of unwanted perturbation have been characterized and measured: electrostatic forces, residual magnetic coupling, damping from residual gas, thermal gradients and so on.

To contribute to this investigation, we are completing a complementary instrument, nicknamed PETER (*Rotational and Translational Pendulum*) (Stanga et al. 2010): a double torsion pendulum where force-free motion has to be achieved simultaneously in two different Degrees of Freedom (DoFs). A description of the apparatus can be found in this volume (Marconi et al. 2012) and in Stanga et al. (2010). Here we recall that a cubic Test Mass (TM) is suspended via two torsion fibres in cascade inside a *Gravitational Reference Sensor* (GRS), that monitors its position through a set of 12 electrodes. The TM motion is almost free (resonant frequencies around 1-2 mHz) for translation of the TM and for rotation around its axis.
PETER will allow us to better represent the flight conditions where the TM is free, and sensitive to forces along all 6 DoFs.

1. Experimental set up and measurements

The displacement of the TM is monitored through linear combination of the output of 6 capacitive-inductive bridges biased at 100 kHz. The relevant observables (corresponding to the two soft DoFs) are the ϕ angle of rotation about the Z (vertical) axis and the position x of the TM center along the X axis. Typical run duration was one to three days. Only the rotation around the x axis was lost because of malfunctioning of one y electrode. In order to explain some "odd" features in our data, not compatible with the basic pendulum model (point mass hanging from an ideal, massless, flexible fibre) , we have developed a model for an extended mass suspended (not necessarily along its symmetry axis) on a thin elastic beam.

Simple pendulum - 1 soft DoF configuration. The apparatus was first operated as a traditional, single DoF torsion pendulum, by fastening the crossbar on a rigid support and keeping the sole lower fibre in operation. For this set-up, we expect to find the torsional motion in the ϕ channel, the swinging motion in x and y channels, and the bouncing motion in the z channel. However, we had to explain the following unexpected features in our data:

– The swinging mode is actually a "doublet" at the frequencies 0.558 Hz and 0.572 Hz. In the time domain, by plotting y vs x, the doublet corresponds to Lissajous figures on the xy-plane and the envelope of these is tilted of about -13 degrees (Fig. 1, left).

–The doublet is also present in the z displacement spectrum: in the simple pendulum swinging, vertical motion is a second order effect and should therefore appear, if at all, at twice the doublet frequencies.

–The spectrum of the ϕ rotation shows, in addition to the torsion line at 2.2 mHz, the doublet of the swinging motion: in other words, the torsional oscillation is modulated at the swinging frequencies. (Fig. 1, right).

Double pendulum - 2 soft DoF configuration. Data were later achieved with the cross-bar released. The torsion frequency of the upper fibre was expected at about 1.4 mHz. Also the spectra of the data recorded in this configuration (2 DoFs) show many couplings among the modes (i.e. the same peaks appear in many channels). However, while for the 1 DoF case model misalignments are necessary to explain the couplings, in the 2 DoFs case the intrinsic complexity of the system, even in absence of misalignments, accounts for most of the observed features (see below).

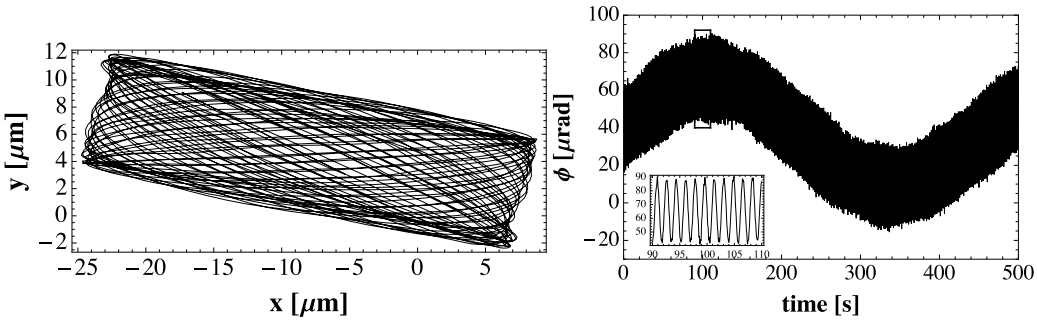

Figure 1. Left: Lissajous figure as described by pendulum data (time span: 80s). Note that x and y axes have different scales. Right: torsion of the TM from data: the modulation at the swinging frequency is clearly visible in the zoom insert.

2. Mechanical models for the pendulum

Modeling of 1 'soft' DoF: extension of the pendulum model. The basic concept of the mechanical model we developed is to consider a rigid body suspended to the fibre at an arbitrary point, not necessarily associated to any particular symmetry of the body: indeed, some misalignment can always occurr when the fibre is fastened to the TM, so that the fibre direction might not coincide with a symmetry axis of the TM.
We describe a system consisting of a thin fibre hanging from a fixed point P_1: at the lower end of the fibre, in the point P_2, at a distance ℓ_0 (along z at rest) a solid, symmetric TM is suspended. The center of mass of the TM is at a distance ℓ_1 below P_2, hopefully, but not necessarily, along the "vertical" principal axis of inertia of the TM (see Fig. 2, left). In our case the TM is a hollow Al cube plus a suspension shaft holding a mirror.

Pendulum motion. In general, the motion of a pendulum consists of a combination of three different kinds of oscillations, that are colloquialy indicated as torsion, swinging and bouncing. The equations describing the corresponding eigenfrequencies are well known (Bassan et al. 2012). In particular, the bouncing of the fibre can be described by a spring-mass system, introducing a spring constant $\kappa_b = \sqrt{EA/\ell_0}$, where E is the Young modulus and A the cross-sectional area of the fibre. For our pendulum, the expected resonances are at 2.2 mHz for

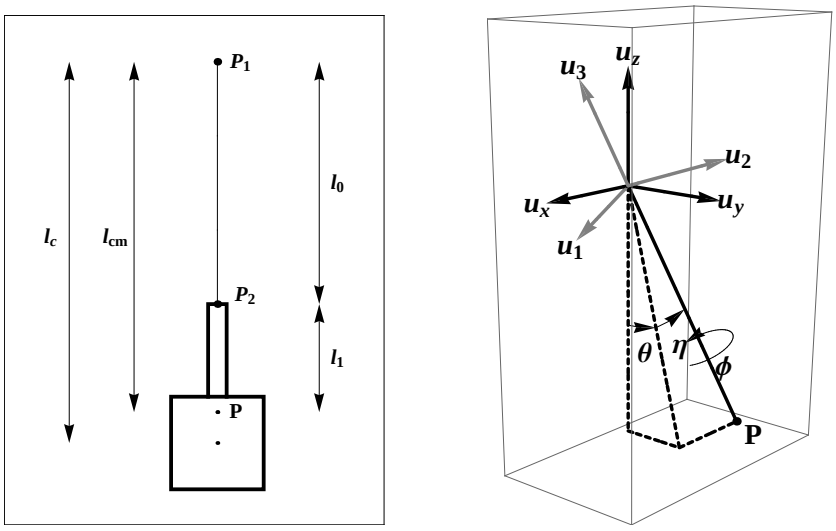

Figure 2. Left: Definition of the lengths mentioned in the text: we neglect here both the dynamic (bouncing motion) and the static elongation of the fibre, P is the position of the center of mass. The center of the cube is also shown, at a distance ℓ_c from P_1. Right: moving coordinate system: u_x, u_y, u_z represent the inertial frame, while u_1, u_2, u_3 identify the coordinate system at rest with the rigid body.

the torsional mode, at 0.56 Hz for the simple, swinging pendulum motion and at 8.8 Hz for the bouncing motion.

In order to describe the pendulum motion, we usefully adopt the system of coordinates (Tu et al. 2004) shown in Fig. 2 (right), noting that they differ from the usual polar coordinates. Using the variables θ, η (motion in the xy plane), ϕ (torsion angle) and δ (elongation of the fibre), we wrote the Lagrangian of the system and obtained the equations of motion. In the ideal case (without misalignments) we get four uncoupled equations ($l_{cm} = l_0 + l_1$):

$$I'_{11}\ddot{\theta} + mg\ell_{cm}\theta = 0; \qquad I'_{22}\ddot{\eta} + mg\ell_{cm}\eta = 0; \qquad I_{33}\ddot{\phi} + \kappa_t\phi = 0; \qquad m\ddot{\delta} + \kappa_b\delta = 0$$

(I_{11}, I_{22}, I_{33} are the principal moments of inertia of the TM[1], while $I'_{11} = I_{11} + m\ell^2_{cm}$ and $I'_{22} = I_{22} + m\ell^2_{cm}$).
The first two equations show that the swinging modes are degenerate if $I'_{11} = I'_{22}$. The third equation shows that ϕ should exhibit harmonic motion at $\omega_t = \sqrt{\kappa_t/I_{33}}$. Likewise, from the fourth relation, δ should move only at the angular frequency $\omega_b = \sqrt{\kappa_b/m}$. However, this is not what we experimentally observed.

We introduce the misalignment angles θ_0, η_0, ϕ_0 and we re-calculate the equations of motion. If $I'_{11} = I'_{22}$, they do not depend on ϕ_0:

$$\begin{aligned}
&I'_{11}\ddot{\theta} + m\,(g\ell_{cm}\theta - \ell_1\theta_0\ddot{\delta}) - \eta_0 q_\theta\ddot{\phi} = 0,\\
&I'_{11}\ddot{\eta} + m\,(g\ell_{cm}\eta - \ell_1\eta_0\ddot{\delta}) + \theta_0 q_\eta\ddot{\phi} = 0,\\
&I_{33}\ddot{\phi} + \kappa_t\phi - \eta_0 q_\theta\ddot{\theta} + \theta_0 q_\eta\ddot{\eta} = 0,\\
&m\ddot{\delta} + \kappa_b\delta - m\ell_1(\eta_0\ddot{\eta} + \theta_0\ddot{\theta}) = 0,
\end{aligned} \tag{1}$$

[1]Numerical values of the parameters for our apparatus are: $\kappa_b = 299.6$ [kg m^2 s^{-2}]; $\kappa_t = 6.77 \cdot 10^{-9}$ [kg m^2 s^{-2}]; $I_{11} = I_{22} = 2.76 \cdot 10^{-4}$ [kg m^2]; $I_{33} = 3.71 \cdot 10^{-5}$ [kg m^2]; $m = 0.106$ kg; ℓ_0=0.65 m; ℓ_1=0.11 m.

where $q_\theta = I_{11} - I_{33} + (\ell_1/\ell_{cm})(I_{33} + m\ell_{cm}^2)$, and $q_\eta = I_{11} - I_{33} + m\ell_{cm}\ell_1$.

Being $I_{33} \ll I_{11} \ll m\ell_{cm}\ell_1$ we assume, from now on, $q_\theta \approx q_\eta \approx m\ell_{cm}\ell_1$.

Note that the introduction of misalignments generates coupling among all variables. The third of eq. (1) shows that the coupling between torsion and swinging arises from both θ_0 and η_0 angles of misalignment. This allow us to explain why we found a modulation of the torsion motion at the swinging frequency.

Finally, the fourth equation contains θ and η: this explains another "feature": the unexpected presence of the doublet in the z spectrum.

With further analysis, we obtain two relations that link the misalignment angles θ_0,η_0 with the splitting of the swinging mode $\Delta\nu$ and the orientation α of the Lissajous figures:

$$\Delta\nu = 10.156\,(\theta_0^2 + \eta_0^2) \quad \text{and} \quad \alpha = -\arctan(\eta_0/\theta_0).$$

From our data $\alpha \approx 13^\circ$ and $\Delta\nu$=14 mHz. This imply $\theta_0 \simeq \pm 36$ mrad, $\eta_0 \simeq \mp 8.4$ mrad.

2 'soft' DoFs configuration: analytic model for PETER. The model for PETER is the natural extension of the 1 DoF model described above. Here, the 'crossbar+ counterweights' component is considered as a rigid body, affected by torsion, swinging, and bouncing (upper fibre), while the TM, with its 4 DoF described above, hangs from the crossbar. 'Rocking' motions of the two rigid bodies are not considered, as they move rigidly together with each fibre: the additional frequencies associated to these relative motions are not observed in the data.

To write the Lagrangian, we set an inertial frame which orientation is as follows: u_z along $-\mathbf{g}$, u_x and u_y along the crossbar arms at the equilibrium point, when no torsion is present (see Fig. 3), and two other frames: the first comoving with the crossbar $(u_{1,a}, u_{2,a}, u_{3,a})$ and the second comoving with the TM $(u_{1,b}, u_{2,b}, u_{3,b})$.

As for the 1 DoF case, we calculate the (linearized) equations of motion in the variables θ_a,

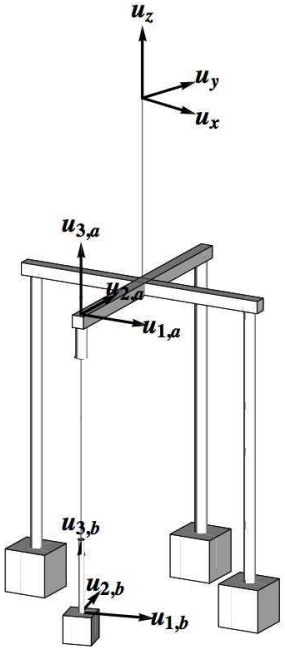

Figure 3. A scheme of PETER with the reference frames described in the text.

η_a, ϕ_a, δ_a, θ_b, η_b, ϕ_b, δ_b, where the suffix 'a' (*above*) is referred to the crossbar+conterweights component and 'b' (*below*) to the TM. Finally, we express the observables $x, y, z, \theta, \eta, \phi$. in

terms of the above described variables.
The equations of motion are then numerically solved to yield the time evolution of the observables, under arbitrary but realistic initial conditions. The spectra of these functions can be compared with those obtained from the data: in Fig. 4 we show, as an example, in three frequency bands, the spectra of ϕ, x, y and z for real (left) and simulated (right) spectra. In the upper, low frequency panels, the torsion modes in ϕ (line) and x (dashed) are shown. In the middle and low panels we show the spectra of x , y and z in two higher frequency bands. The peak at 0.4 Hz corresponds to the crossbar+counterweights swinging frequency and it appears in all 3 channels, while that at 0.58 Hz, a swinging of the TM, is not seen in x. These and other non obvious features are well reproduced by the simulation. We note however that the swinging peak at 0.61 Hz is not present in the y and z simulated channels. This discrepancy probably arises from neglecting misalignments.

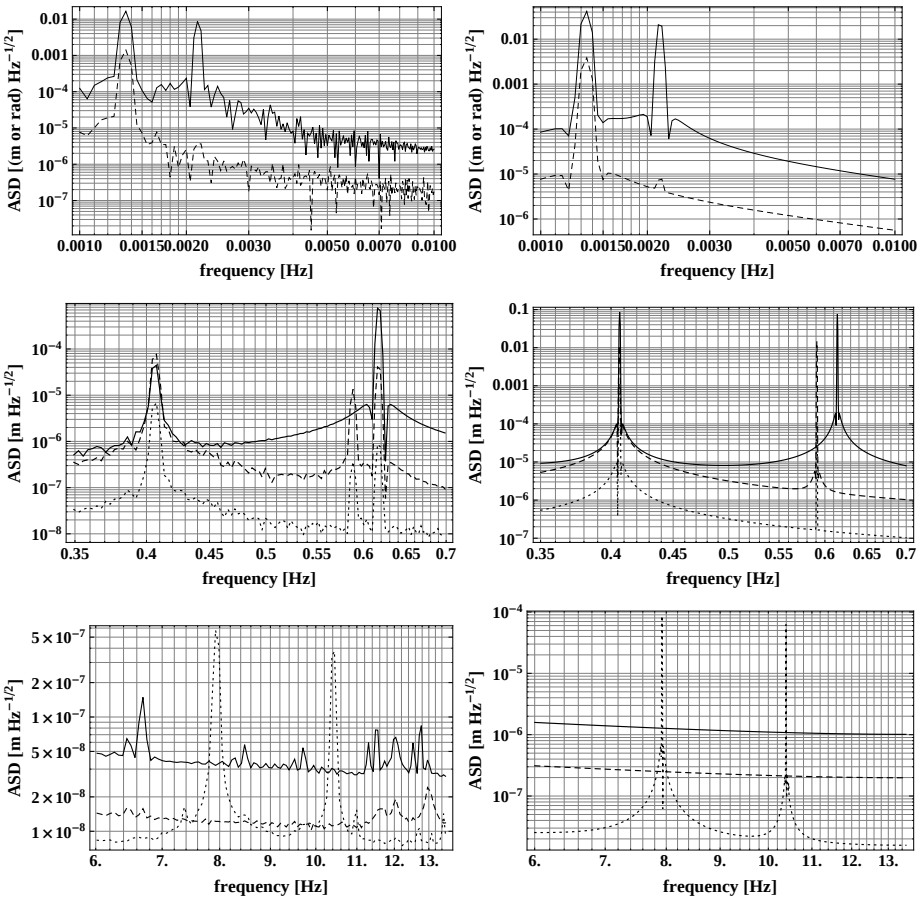

Figure 4. Data from the double pendulum (left) compared to our simulation (right). Upper panels: ϕ (solid line) and x (dashed line); the peaks correspond to the torsion modes (units are: meters for x and radiants for ϕ). Middle and lower panels: spectra of x (line), y (dash) and z (dotted) at higher frequencies. In the lower panels the two peaks in z correspond to the bouncing resonances.

Conclusions. A double pendulum is an important tool to test 'almost free' motion on more than one degree of freedom. The PETER apparatus was built with this purpose. Due to the

complexity of the experimental apparatus, analysis of its data requires a deeper understanding of its mechanics. We have developed a model that explains, on pure geometrical basis, several odd features found in our 1 DoF pendulum data. A detailed analysis of the geometry of the Test Mass and its suspension for a non ideal case leads to coupled equations of motion that simply explain the unexpected couplings. We then extended our model to the 'complete' PETER neglecting, for the time being, possible misalignments. The numerical solution of the equations of motion shows a good agreement with the observed spectra in the relevant frequency range. In this case, the splitting of the swinging TM modes naturally arises from the complexity of the system, and does not need geometric imperfections to be explained.

Acknowledgments. We thank L. Di Fiore, R. De Rosa and F. Garufi for useful discussions. Continued advice and support from the Trento LISA-Pathfinder group, and in particular from W.J.Weber, is appreciated. Work supported by MIUR (grant PRIN 2008) and by INFN.

References

Bassan, M., et al. 2012, Torsion pendulum revisited. Submitted
Carbone, L., et al. 2005, Class. Quantum Grav., 22, 509
— 2006, Class. Quantum Grav., 873, 561
Marconi, L., et al. 2012, in Proceedings of the 9th International LISA Symposium
McNamara, P., et al. 2008, Class. Quantum Grav., 25, 114034
Pollack, S., et al. 2010, Phys. Rev. D, 81, 021101
Stanga, R., et al. 2010, Journal of Physics: Conference Series, 228, 012037
Tu, Y., et al. 2004, Physics Letters A, 331, 354